Models for the Surface Adsorption of Triblock Copolymers

Anna C. Balazs* and Stephen Lewandowski†

Materials Science and Engineering Department, University of Pittsburgh, Pittsburgh, Pennsylvania 15261. *Received June 29, 1989; Revised Manuscript Received August 11, 1989*

ABSTRACT: Amphiphilic polymers are macromolecules that contain two types of segments: one that is compatible with a solvent and another that is solvent incompatible. In solution, the solvent incompatibility drives parts of the chain to adsorb onto the nearest surface or interface. Once bound to the surface, the presence of the polymer modifies the properties of the interface. However, the ability of these chains to adsorb onto a surface is complicated by the fact that the solvent-incompatible moieties will also associate with each other, causing the chains to self-assemble. Furthermore, chains attached to the surface can associate with free chains in solution. These interactions give rise to a complex microstructure in the interfacial region. In order to examine this microstructure, we develop computer simulations to model the adsorption of ABA triblock copolymers. Here, the A moieties are hydrophobic and the B segment is hydrophilic. Using these models, we examine the conformations of the adsorbed chains. In addition, we investigate how surface coverage is affected by the length of the B segment, polymer concentration, the energy of interaction between the B segment and the surface, polydispersity, and reversible adsorption.

Introduction

The interfacial properties of amphiphilic polymers make them a crucial component in a wide of variety of technological applications, from the steric stabilization of dispersed particles, to the stabilization of oil/water emulsions.[1] Amphiphilic polymers contain two types of segments: one that is compatible with a solvent and another that is solvent incompatible. Solvent incompatibility provides a good mechanism for anchoring segments of the chain onto a substrate. For example, the hydrophobic effect[2] drives the nonpolar moieties (hydrophobes) away from the aqueous environment and onto an available surface or interface. Once bound to the surface, the presence of the polymer modifies the properties of the interface. This phenomenon gives rise to the commercial utility of long-chain amphiphiles. However, the picture is complicated by the fact that the hydrophobes will bind not only to the surface but also to other hydrophobes in the solution. This situation is familiar for the case of simple diblock architectures, where above a critical concentration, distinct micelles are formed in the solution.[3-5] However, as the polymer architecture becomes slightly more complex (consider a triblock composed of a hydrophilic segment capped by two hydrophobic end groups), the ability of these molecules to self-assemble will further affect their interactions with the surface. As will be seen in the forthcoming figures, now actual structure *within* the interfacial region is also influenced by the association reactions between the triblocks. In order to profit from the interfacial properties of the more complicated amphiphiles it is crucial to understand how their surface adsorption is affected by these self-assembling reactions. Below, we report on the results of using Monte Carlo simulations to examine the surface adsorption of self-assembling triblock copolymers.

Computer simulations provide both a qualitative and quantitative means of understanding the factors that influence polymer–surface interactions. First, by viewing the graphical output throughout the course of the simulation, one can actually "watch" the molecules adsorb onto the surface and actually "see" the intricate microstructure evolve. This level of visualization is invaluable for unraveling the complex series of events that occur at the interface. Second, the quantitative features that characterize the interfacial region are easily computed. Such features include the fraction of polymers bound to the surface and in all subsequent layers (i.e., the polymer segment density profile), the layer thickness, and the conformation and dimensions of the bound (and free) chains. These parameters can be evaluated at any point in the reaction. Consequently, the data yield information on the kinetics of adsorption, as well as knowledge about the final equilibrium state. This point is particularly important since recent kinetic studies[6] indicate that while the initial surface adsorption of diblock copolymers is rapid, the equilibrium adsorbance is reached only at much longer times. Thus, experimental measurements made after polymers and the surface have been in in contact for only short times (<10 h[6]) may be more revealing of the kinetic behavior than the final equilibrium state. Consequently, understanding the kinetic effects may be extremely helpful in explaining observed trends. Third, computer "experiments" to systematically alter various polymer or surface properties are easily carried out, and hence, we can readily examine how such variations affect the adsorption process.

In problems involving the reactions of self-assembling molecules, computer simulations also provide a significant advantage over analytical models. In using an analytical approach, one is forced a priori to assume a particular geometry not only for the clusters of aggregated molecules but also for the microstructure at an interface.[7] Since these microstructures are highly complex or yet uncharacterized, analytical models are not well suited for studying this class of problems.[8] In simulations, on the other hand, no assumptions are made about the geometry of the interface (or the aggregates): the molecules are allowed to adsorb and self-assemble into whatever microstructure they prefer. Thus, simulations address the limitations of the analytical approach.

Below, we describe the computer model we developed to examine the surface adsorption properties of ABA triblock copolymers. The A blocks represent the "sticky" hydrophobic segments (or "stickers"), while the B segment models an internal hydrophilic block. In a previous study,[9] we investigated the ability of these molecules to self-assemble in solution. In particular, the chains

† Current address: Mobay Corporation, Bayer USA Inc., Pittsburgh, PA 15205-9741.

0024-9297/90/2223-0839$02.50/0

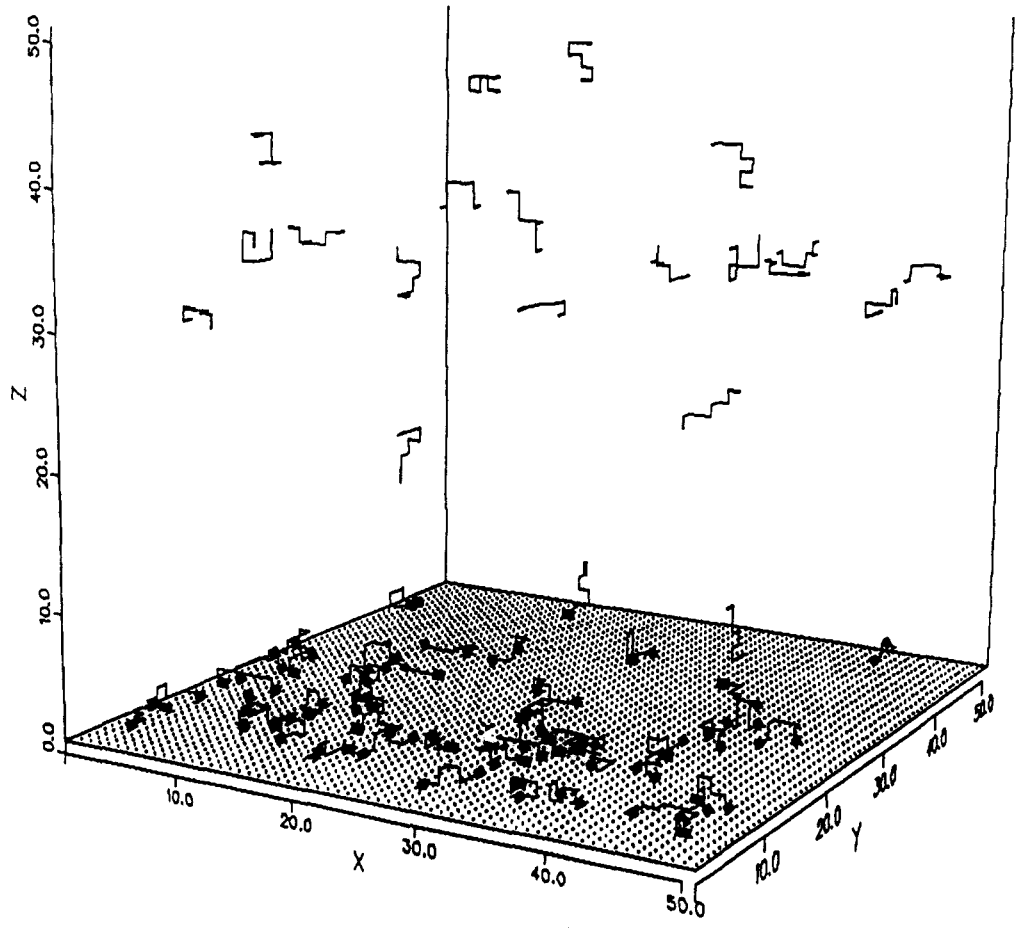

Figure 1. Graphical output from the 3-D simulations. The $z = 0$ plane represents the adsorbing surface. The chains in the upper half of the cube are free chains in solution. The hydrophobes on the bound chains are drawn with a thick line so as to distinguish readily the polymers attached to the surface. Here the chains are 10 lattice sites in length.

associate through the A moieties to form extensive clusters or networks. Here, we are interested in examining how these chains behave near an interface. Specifically, we examined the effect of the following parameters on surface adsorption: length of the B block, polymer concentration, A–A type associations, the interaction energy between a B segment and the surface, and polydispersity in molecular weight.

The Model

The current simulation is started by randomly introducing a specified number of chains into a cubic volume with 50 lattice sites on a side. These chains represent the "free" macromolecules in solution; the number of these free chains is held constant throughout the simulation. The scenario that our simulation models is one in which the solution is in contact with and lies directly above an adsorbing surface. Consequently, the bottom plane ($z = 0$) of the cubic lattice represents the surface to which the polymer molecules can diffuse and adsorb.

The polymer chains are composed of n lattice sites and the last bond, on both ends of the chain, represents the A block. As in the previous study,[9] the chains bind through these A segments. In particular, a chain becomes adsorbed to the surface (or attached to another chain in the adsorbed layer) when one of the A stickers is parallel to and one lattice site away from the surface (or from a sticker on an adsorbed chain). Presently, the length of the A region is kept fixed and the chain length is varied by modifying the length of the internal B block.

At the beginning of the simulation, one of the free chains is picked at random and allowed to execute a self-avoiding random walk. The random walk is composed of two parts: a translation and a "wiggling" motion. The translation consists of moving the entire chain one lattice site in a direction to be picked at random: either up, down, right, left, forward, or backward. Then, the wiggling, or chains dynamics, is simulated by using the Verdier–Stockmayer algorithm,[10] with the corrections suggested by Hilhorst and Deutch.[11] Each motion is attempted and is accepted only if it meets the excluded-volume criteria. This procedure is repeated until an A segment is aligned parallel to and one lattice site above the surface. The A segment then remains stuck at this position; however, the remaining portion of the chain is free to wiggle. A chain that has one stationary end is referred to as "partially frozen". At this point, a new chain is added to the solution, thus keeping the number of chains in the bath constant. (Here, the solution acts as an infinite source of free chains.)

Now, a chain is again picked at random. If the partially frozen chain is picked, it is free to wiggle, while a free chain can translate and wiggle. This procedure is repeated until one of the following bonding events occurs: (1) an A segment on a free chain bonds to the surface, (2) this segment bonds to the free A end on a partially frozen chain, or (3) the free A end on a partially frozen chain binds to the surface. In cases (1) and (2), a new chain becomes partially frozen, and an additional chain is added to the bath. In case (3), both A segments have become bound, thus a partially frozen chain becomes completely "frozen": the entire chain remains fixed in location. In the latter event, no new chain is added to the solution. Eventually both ends of a chain may be paired

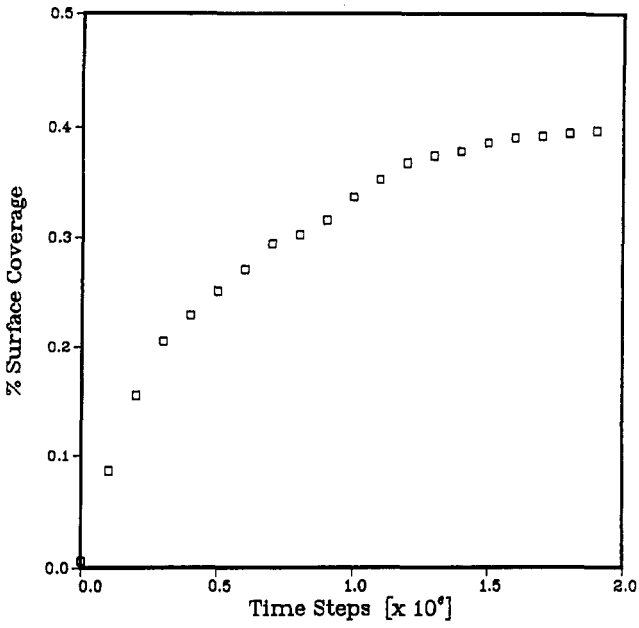

Figure 2. Surface coverage versus computer time steps (chain length = 20, P_R = 0.0, P_{A-A} = 1.0, χ_{AS} = χ_{BS} = 0.0, number of free chains = 20).

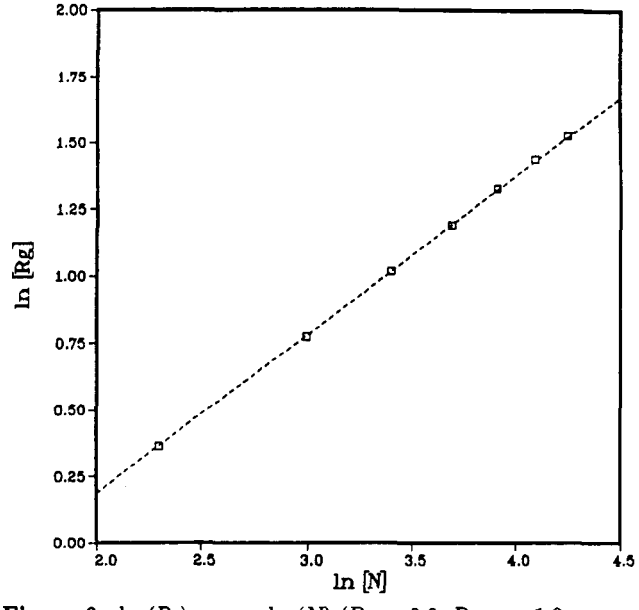

Figure 3. ln (R_g) versus ln (N) (P_R = 0.0, P_{A-A} = 1.0, χ_{AS} = χ_{BS} = 0.0, number of free chains = 20). Slope = 0.594.

with ends on other chains, the polymer having been "trapped" and, in turn, trapping another chain from reaching the surface. In this case, as well, the chain is considered "frozen".

Since we wish to focus attention on the character and growth of the adsorbed layer, we will not allow free chains to associate among themselves. (Their aggregation has been described in a previous paper.[9]) To summarize, a free chain can bind to the surface or to a chain that is already adsorbed, i.e., that is partially frozen or frozen.

Both reversible and irreversible[6,12] adsorption have been proposed as realistic possibilities for describing polymer–surface interactions. In the majority of the simulations described below, the binding between an A segment and the surface, as well as the bindings between different A segments, is assumed to be irreversible. However, various results from a reversible-binding model are also presented. In this version of the simulation, bonding occurs as outlined above; however, at some later time step, the most labile chains are allowed to break away with a prescribed probability "P_R". The most labile polymers are the partially frozen chains that are linked to the interfacial region by only one bond. Chains bound through two or more bonds are clearly less likely to desorb than a singly bound species. If a chain leaves the surface layer, in another time step it may either rejoin this layer or diffuse further away.

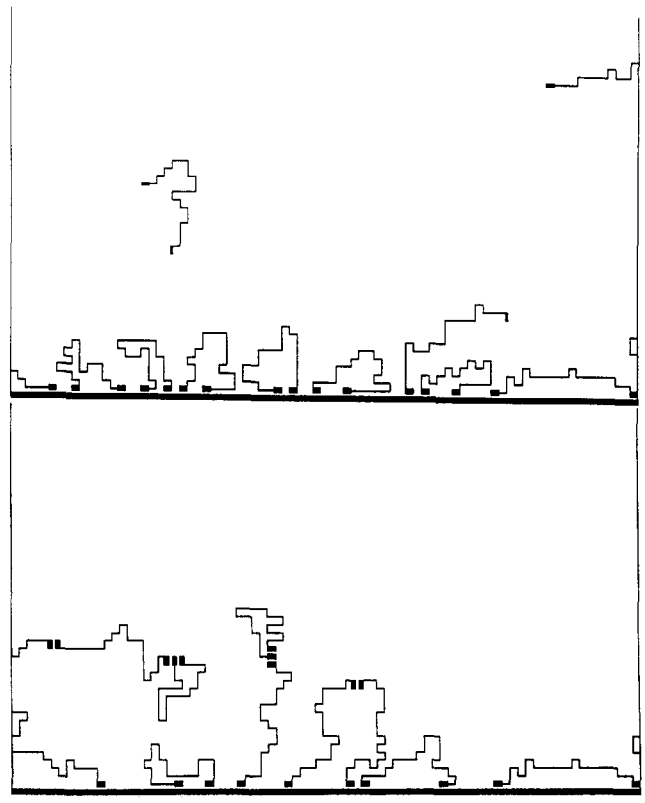

Figure 4. Conformation of bound chain for P_{A-A} = 0.0 (top) versus P_{A-A} = 1.0 (bottom) (P_R = 0.0, χ_{AS} = χ_{BS} = 0.0, number of free chains = 20, chain length = 30). Only a portion of the entire surface is shown.

The simulations are carried out in both two and three dimensions. The three-dimensional model is a far more realistic representation; however, the figures generated from the two-dimensional simulations are easier to interpret than the images obtained from the 3-D calculations. Consequently, the 2-D diagrams are useful for gaining a qualitative understanding of observed trends. Figure 1 shows the graphical output from a 3-D simulation, while subsequent diagrams will show the 2-D images. Finally, we note that the calculations can be halted after a specified number of time steps or when a specified number of chains have been incorporated into the adsorbed layer.

Results and Discussion

We are interested in the microstructure of the adsorbed layer after a significant number of macromolecules have been adsorbed onto the surface. Therefore, it is important to describe when, during the course of a simulation, measurements were made. Figure 2 shows surface coverage (the fraction of surface sites occupied by polymer), θ, versus computer time steps for the irreversible adsorption of a monodisperse sample of chain length 20. The general shape of the curve coincides with experimental observations on the kinetics of diblock adsorption.[6] Here, as the number of time steps nears two million, the fraction of surface lattice sites bearing adsorbed polymer

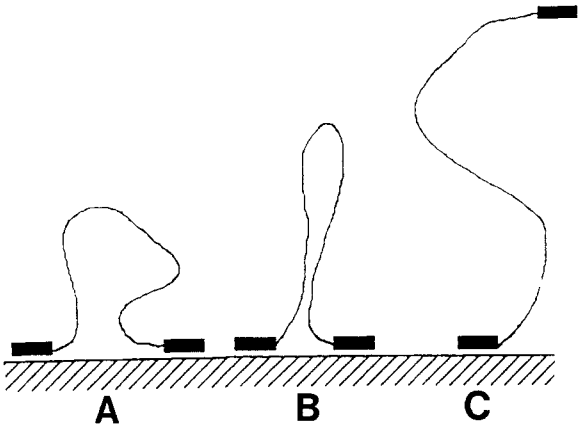

Figure 5. Conformation of bound chains for $P_{A-A} = 0$: (A) at short times and low surface coverage, (B) at intermediate times, surface coverage $>C^*$, and (C) at long times and high surface coverage.

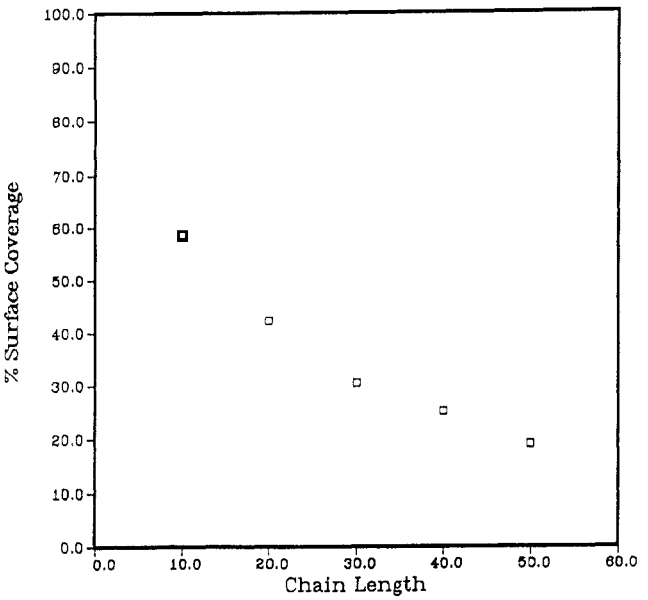

Figure 6. Surface coverage versus chain length ($P_R = 0.0$, $P_{A-A} = 1.0$, $\chi_{AS} = \chi_{BS} = 0.0$, number of free chains = 20).

as the number of time steps nears two million, the fraction of surface lattice sites bearing adsorbed polymer reaches a plateau. Past two million time steps, surface coverage increases by only 1–2% per million time steps. All of our measurements were made at four million time steps. This puts us well onto the region where changes in the number of chains adsorbed are occurring at a very slow rate and well within the limitations of reasonable computational time. The numerical results presented are averages obtained from running each simulation in triplicate. All values were obtained from the three-dimensional model. Images from simulations run in two dimensions are presented only to help explain the observed trends.

The dimensions of the adsorbed chains, radius of gyration, and extension normal to the surface or layer thickness (L) are critical to determining the ability of the adsorbed chains to impart steric stabilization. To determine the behavior of these parameters, we performed a series of simulations in which we systematically varied the length of the chain, N. For each of these N values, the radius of gyration, R_g, for the adsorbed chains was calculated. We then plotted natural log (R_g) versus natural log (N). The slope of this line yields the value of

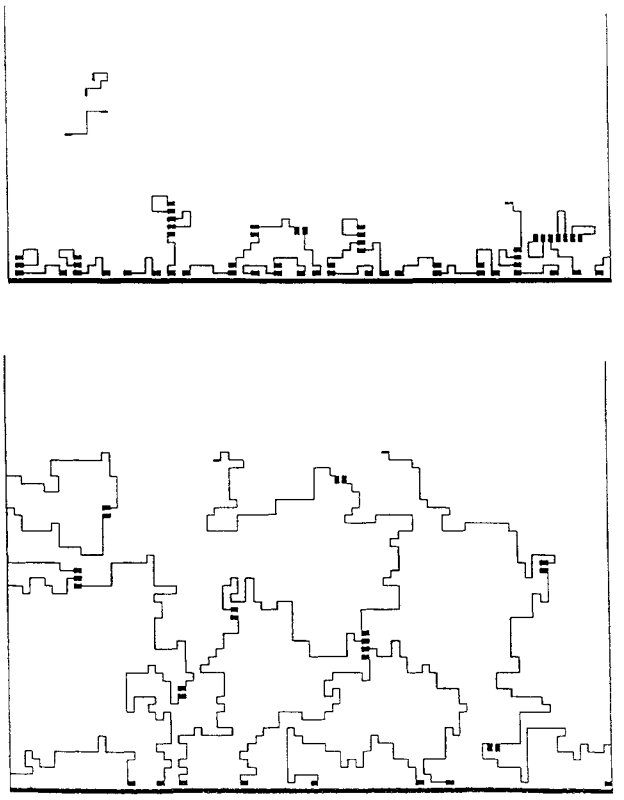

Figure 7. Two-dimensional images of adsorbed layers composed of short chains (10 lattice sites, top) and long chains (50 lattice sites, bottom).

the scaling exponent, ν, relating the two variables:

$$R_g = aN^{\nu} \tag{1}$$

We obtain a value of $\nu = 0.594$ (Figure 3), which agrees extremely well with the value of 3/5 or 0.6 predicted by Flory for self-avoiding random walks in 3-D.[13]

Using the data from Figure 3, we determined the value for a in eq 1. From a known value of R_g, we can calculate the value for the concentration of bound chains at the overlap threshold, C^*, the surface density at which these chains just begin to overlap:[14-16]

$$C^* = 1/\pi R_g^2 \tag{2}$$

These calculated values are compared with the surface concentrations obtained after four million time steps in Table I. The surface concentrations from the simulations are very close to C^* for all lengths, except chain length 10. For a chain length of 10, surface concentration is significantly less than C^*. These results and the shape of the plot for surface coverage versus time (Figure 2) indicate that, for most chain lengths, the adsorption process proceeds quite readily up to a surface concentration near C^*. Beyond this point, it becomes increasingly more difficult to adsorb new macromolecules, since both attached and "attaching" chains must become more and more stretched from their entropically favorable random coil conformation. However, running the simulations for significantly more time steps does yield surface concentrations above C^*. (Results at high surface coverage will be discussed in a future paper.) Again, this result coincides with the kinetic studies on diblocks: the first stage of the adsorption occurs rapidly, followed by a slow adsorption process at long times.[6]

Returning to our observations for short chains, the surface concentration is restricted by a trapping mecha-

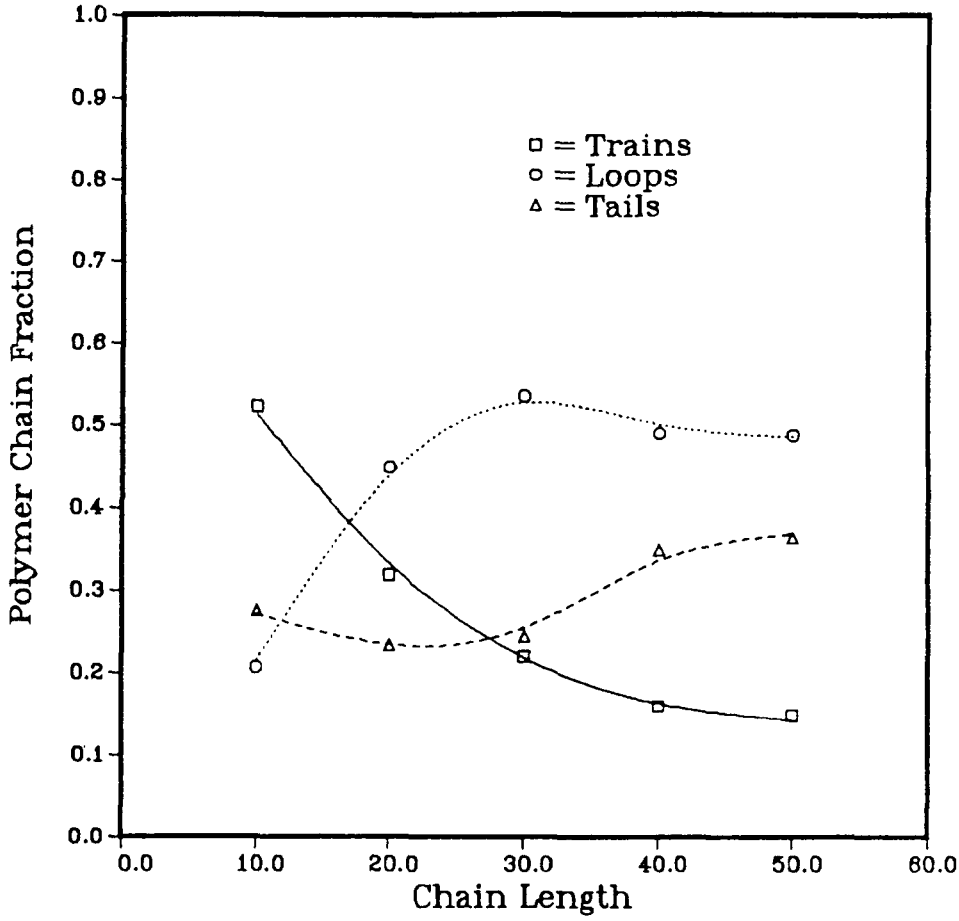

Figure 8. Train, loop, and tail, analysis after four million time steps for several polymer chain lengths (P_R = 0.0, P_{A-A} = 1.0, χ_{AS} = χ_{BS} = 0.0, number of free chains = 20).

nism. A large percentage of each short chain is sticky. If a free chain approaching the surface collides with an adsorbed short chain, it is likely to be captured by the adsorbed chain and prevented from continuing on toward the surface. A much lower percentage of the chain is sticky for longer chain lengths. Therefore, approaching chains are more likely to collide with and "bounce off" adsorbed chains and continue to the surface.

A ln–ln plot of layer thickness, L, versus chain length was also examined. (In our measurements for L, we only consider chains bound directly to the surface.) The slope, or scaling exponent, of 0.649 is slightly higher than the theoretical value of 3/5 for surface concentrations at or below C^*. Thus, the conformations of the adsorbed chains are slightly elongated in the direction normal to the surface. This elongation can be understood by comparing these results with those obtained from chains that can adsorb onto the surface but do not self-associate.

Examination of chains that do not self-assemble was carried out by setting P_{A-A}, the probability of a sticker–sticker association, equal to 0.0. The probability of sticker–surface attachment remains unchanged at 1.0. In this way, the chance for surface adsorption has not been changed, but free, frozen, and partially frozen chains can no longer associate among themselves. Once again, ln (R_g) and ln (L) were plotted against ln (N). The scaling exponents relating R_g to N and L to N are 0.579 and 0.583, respectively. Both agree with the theoretically derived relationship $R_g \sim N^{3/5}$. When self-assembly is forbidden, L shows no chain stretching normal to the surface.

The differences in L values for the associating and nonassociating chains at surface coverages comparable to C^* are attributable to the possible conformations the chains can assume at the interface. For the case of nonassociating chains, the only interactions occur between the surface and an A segment. At C^*, most chains occupy roughly a half-sphere, with both associating sites bound to the surface. However, for the self-assembling species, a chain attached at one end can still associate with chains in solution via its other A segment. Thus, these chains are stretched away from the surface through their interactions with chains in solution. These effects become more pronounced at longer chain lengths. The contrasting conformations can be seen in the 2-D images in Figure 4. These results clearly show that self-association reactions affect the configuration of surface-bound chains, as well as the microstructure of the interfacial region.

Previous theoretical work pertaining to the layer thickness of diblock copolymers grafted or adsorbed onto a surface at high surface densities shows that $L \sim N$.[16,17] For irreversibly bound, nonassociating ABA triblocks, the scaling exponent will always be less than 1. Figure 5 provides a qualitative way of understanding this observation. At low surface coverage, the chains bind with both A segments attached to the surface, extending in a lateral and vertical distance that is comparable to $R_g \sim N^{3/5}$ (Figure 5A). As the surface becomes more crowded, there is less space available to which the chains can bind. At this stage, the chains are more likely to bind in the hairpin configuration seen in Figure 5B, where the chain is stretched in the vertical direction and occupies less space on the surface. Eventually, there is insufficient space for both A segments to bind and the last chains to attach are bound in the "tail" conformation seen in Figure 5C.

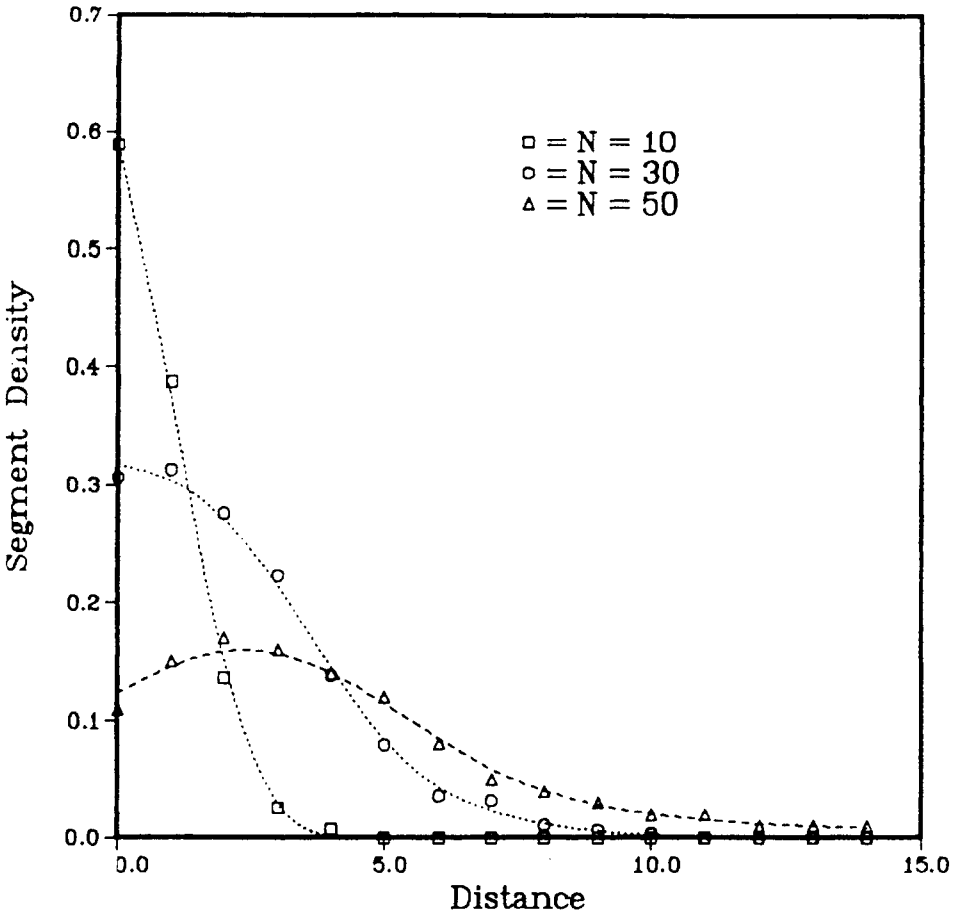

Figure 9. Polymer segment density (volume fraction) versus distance from the adsorbing surface (P_R = 0.0, P_{A-A} = 1.0, χ_{AS} = χ_{BS} = 0.0, number of free chains = 20).

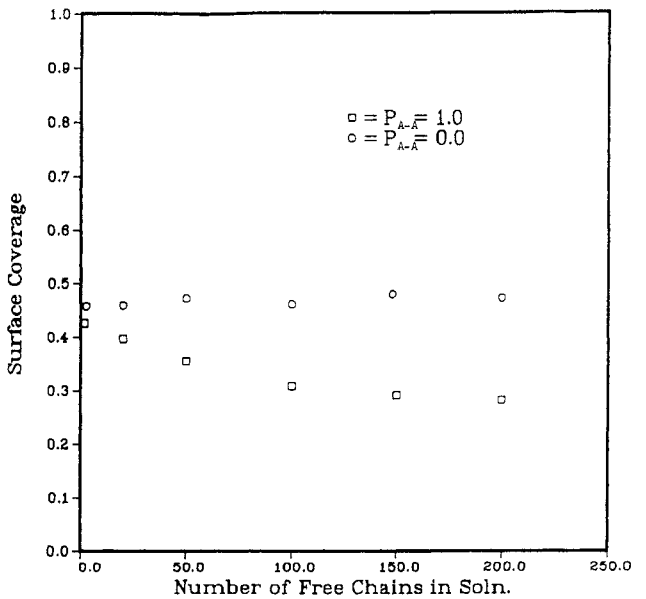

Figure 10. Surface coverage versus chain length when self-assembly occurs, P_{A-A} = 1.0, and when chains do not associate among themselves, P_{A-A} = 0.0 (P_R = 0.0, χ_{AS} = χ_{BS} = 0.0, number of free chains = 20).

Thus, the scaling behavior of L is bimodal as a function of time: the first chains to bind display $L \sim N^{3/5}$ behavior, while the chains that bind later in time will exhibit $L \sim N$ character. Experimental measurements of the average layer thickness at high surface coverage will include contributions from both the early and late stages of surface adsorption. Consequently, they will yield a value that is an average of these components, in other words, a value of the scaling exponent that lies between 3/5 and 1. These observations are consistent with preliminary experimental measurements for the adsorption of PVP–PS–PVP triblocks onto mica from a selective solvent (toluene). Here, at high surface coverage, the scaling exponent relating L to N was found to be less than 1.[18]

Having determined the conformation of the attached chains, we next investigated how various conditions affect the adsorption behavior. In particular, the length of the B block was systematically increased to observe the effect of chain length on surface coverage for the self-assembling ABA triblocks. As Figure 6 shows, surface coverage decreases dramatically as chain length increases. Similar results have been observed for AB diblocks,[6,19] where the short A segment was again the surface-binding moiety. This trend can be understood by examining the two-dimensional images in Figure 7. For short polymers, a high fraction of contiguous segments lie directly on the surface, in what is referred to as a "train" conformation. However, as the length of the nonbonding B block is increased, a higher fraction of the chain segments lies away from the surface, in "loop" or "tail" configurations (see Figure 8). (In the former case, a section of the chain lies above the surface, pinned between two bound regions. The "tail" refers to a free end in solution, which is attached to the surface through the other end of the chain.) These long flexible tails can sterically hinder or trap other chains from adsorbing onto the surface. Thus, both statistical and steric hindrance arguments account for trends in Figures 6 and 7.

The simulations also provide valuable information on the amount of polymer in all the adsorbed layers, not

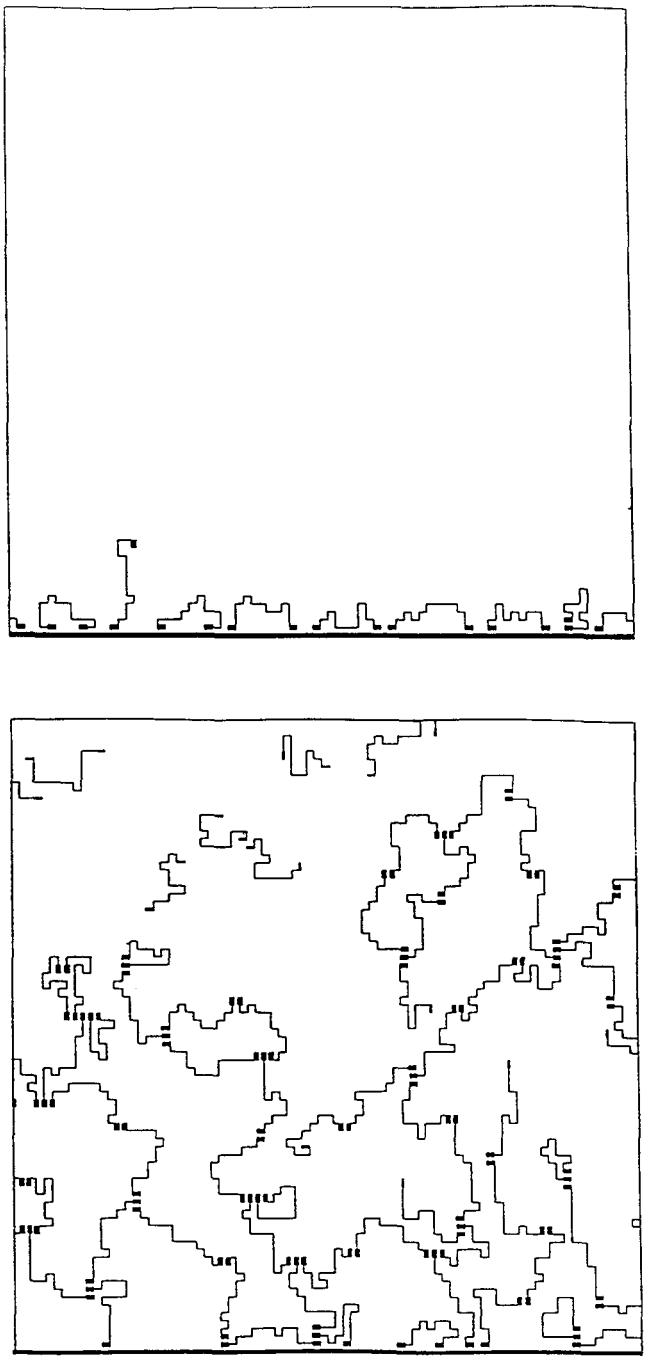

Figure 11. Top: Adsorbed layer obtained from dilute solution (P_{A-A} = 1.0, P_R = 0.0, χ_{AS} = χ_{BS} = 0.0, number of free chains = 2). Bottom: Adsorbed layer obtained from concentrated solution (P_{A-A} = 1.0, P_R = 0.0, χ_{AS} = χ_{BS} = 0.0, number of free chains = 200).

just the surface layer. Figure 9 shows the polymer segment density profile as a function of distance from the surface. The plot shows these curves for chain lengths 10, 30, and 50. These figures again illustrate the fact that surface coverage decreases as a function of chain length. As expected, the width of the entire interfacial region is greater for longer chains.

We also investigated the effect of polymer concentration in the solution on the surface coverage. The length of the chain was held constant at 20 lattice sites; however, the concentration of free chains was varied. Here, the specified number of free chains is held fixed throughout the course of a particular simulation. Values between 2 and 200 were examined in the different simulations. A series of calculations were performed for both the associating and nonassociating polymers. Figure 10 shows the variation in surface coverage with the number of free chains in solution. Over the concentration range studied, surface coverage decreases with increased solution concentration only when self-assembly is permitted. When polymer chains are not allowed to self-associate, surface coverage shows a slight increase with an increase in solution concentration. The latter behavior can be understood by noting that the more free chains in solution, the more chains that will be located near the interface and, consequently, these chains will take less time to diffuse to the surface. Thus, for a fixed amount of time, there will be a higher surface coverage for a higher solution concentration.

Table I
Surface Concentration of Adsorbed ABA Polymer Molecules for Various Chain Lengths[a]

chain length	$R_g = 0.361(N)^{3/5}$	C^*, chains/unit area	$C_{(sim)}$
10	1.44	0.154	0.112
20	2.17	0.067	0.066
30	2.78	0.041	0.046
40	3.30	0.029	0.029
50	3.37	0.022	0.024

[a] P_{A-A} = 1.0, P_R = 0.0, χ_{AS} = χ_{BS} = 0.0, number of free chains = 20.

Figure 11 yields a qualitative means of understanding the former behavior. As the solution concentration increases, the free A end of a bound chain is more likely to interact with an A segment in solution and less likely to loop back to the surface. This interaction effectively traps incoming chains from ever reaching the surface. As the reaction proceeds, the trapped chains form a surface-shielding network that sterically hinders other chains from reaching this destination. We note that this behavior is a kinetic effect that will be particularly apparent in the cases where the lifetime of the A–A association is long compared to the diffusion rate of a chain to the interface. If this lifetime is short, a trapped chain will eventually break away and continue to diffuse toward the surface. In this case, the final equilibrium state will reveal a surface coverage that does *not* decrease with an increase in polymer concentration.

Another parameter that can effect the degree of surface coverage is the energy of interaction between the internal B segment and the surface, or χ_{BS}. Here, we assume that the interaction energy between the A moiety and surface, χ_{AS}, is sufficiently strong that this segment will bind to the interface whenever geometrically possible. We are particularly interested in the case where $\chi_{BS} > 0$ and $\chi_{AS} = 0$, i.e., the B–surface interaction is repulsive while the A–surface interaction is attractive. In the version of the simulation used to examine this issue, the chains are allowed to adsorb as described above, however, we now count the number of B segments that are also in contact with the surface. This configuration is weighted by the factor $q = \exp(-n\chi_{BS})$, where n is the number of B segments on the surface and χ_{BS} is ≥ 0.[20] Specifically, a number is obtained via the random number generator: if its value is less than or equal to q, the chain conformation is maintained; if the random value is greater than q, the chain is returned to the location it had in the previous time step. Figure 12 shows the segment density profiles for the adsorption of a monodisperse sample of chain length 30 for χ_{BS} = 0.10, 0.20, 0.50, and 1.00. Increasing χ_{BS} (greater B–surface repulsion) lowers the polymer segment density in the surface layer. The polymer is now more concentrated in the second and third layers of the film. The appearance of a maximum

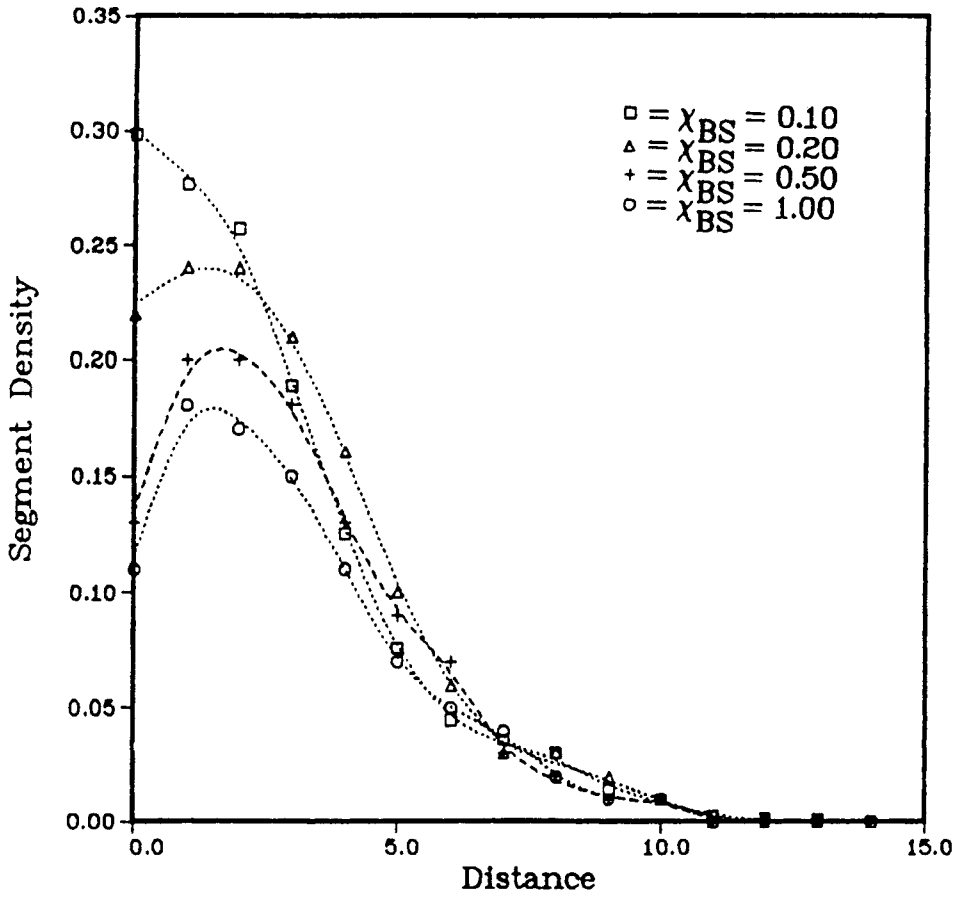

Figure 12. Segment density profiles for several values of χ_{BS} (P_{A-A} = 1.0, P_R = 0.0, χ_{AS} = 0.0, number of free chains = 20, chain length = 30).

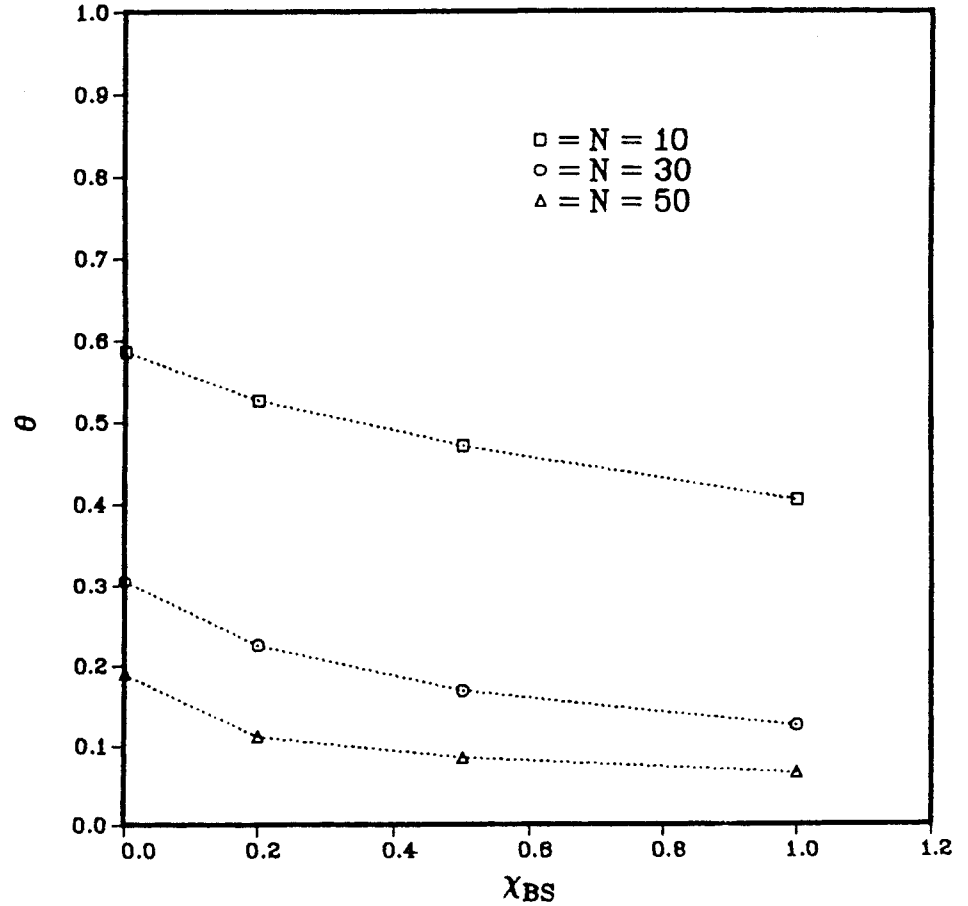

Figure 13. Surface coverage versus χ_{BS} (P_{A-A} = 1.0, P_R = 0.0, χ_{AS} = 0.0, number of free chains = 20, chain lengths = 10, 30, and 50).

Table II
Molecular Weight Distribution of the Directly Adsorbed Chains for Several Heterodisperse Samples[a]

sample	chain length	no. fractn in soln	mobility	no. adsorbed calcd	no. adsorbed sim	surface coverage
1	10	0.75	1.000	224	197	0.66
	30	0.25	0.518	39	29	
2	10	0.50	1.000	126	128	0.45
	30	0.50	0.518	65	58	
3	10	0.25	1.000	54	61	0.37
	30	0.75	0.518	84	81	
4	10	0.50	1.000	102	116	0.38
	50	0.50	0.381	39	42	
5	40	0.50	0.436	31	29	0.17
	60	0.50	0.342	24	26	
6	20	0.50	0.660	64	66	0.31
	40	0.50	0.436	42	41	
7	10	0.282	1.000	61	59	0.36
	20	0.231	0.660	33	29	
	30	0.205	0.518	23	25	
	40	0.154	0.436	14	14	
	50	0.128	0.381	11	10	

[a] $P_{A-A} = 1.0$, $P_R = 0.0$, $\chi_{AS} = \chi_{BS} = 0.0$, number of free chains = 20.

in polymer volume fraction at this location is clearly seen in Figure 12. This trend coincides with observations made by Cosgrove et al.[20] on terminally attached homopolymers. Figure 13 compares the decrease in surface coverage with increasing χ_{BS} for chain lengths 10, 30, and 50. The trend is uniform for all chain lengths examined. The more positive values of χ_{BS} cause the B chain segments to be repelled from the surface. This forces the adsorbed chains into loop and tail conformations that extend away from the surface and consequently decrease surface coverage.

Most practical applications of polymer adsorption involve use of samples with some breadth to their molecular weight distribution. Polydisperse systems are created by specifying the number of chains of a given length that are to be added to the solution. When a chain of a particular length is adsorbed, a new chain of the same length is added to the solution. Thus, the initial distribution of chain lengths is maintained throughout the simulation. The relative mobility of the polymer chains is weighted to reflect differences in molecular weight. Mobility is assumed to be inversely proportional to the radius of gyration of the polymer chain.[21] The frequency with which polymer chains are allowed to translate is weighted by this mobility. The mobility for chain length 10 was assigned a value of 1.000, with longer chains having a lower mobility given by the formula

$$\mu_i = \frac{1/R_{g,i}}{1/R_{g,10}}\mu_{10} \tag{3}$$

$$\mu_i = R_{g,10}/R_{g,i} \tag{4}$$

where $R_{g,i}$ is the radius of gyration for chain length i, $R_{g,10}$ is that for chain length 10, and μ is the corresponding mobility. The simulation has the versatility to maintain any molecular weight distribution.

The molecular weight distribution and surface coverage for several heterodisperse samples are shown in Table II. As would be expected, samples with high proportions of short chain lengths give the highest surface coverage. Also displayed are the relative mobilities of chains of various lengths and the number of chains adsorbed.

We can derive a simple set of equations to predict the number and lengths of chains that will adsorb at the overlap threshold and then compare these values with those measured from the simulation. For a given solution containing polymer chains of two different molecular weights, the ratio of the number of chains of length i and j, n_i/n_j, adsorbed on the surface is

$$n_i/n_j = X_i\mu_i/X_j\mu_j \tag{5}$$

where X is the number fraction of a given chain length in solution. The number of i and j chains that can be most efficiently accommodated by the surface, at the overlap threshold, is given by

$$S = (n_i)(\pi)(R_{g,i})^2 + (n_j)(\pi)(R_{g,j})^2 \tag{6}$$

where S is the total available surface area. The maximum number of i and j chains present on the surface at the C^* concentration can be found by simultaneous solution of eqs 5 and 6 for n_i and n_j. Similar reasoning can be used to calculate the molecular weight distribution of surface-adsorbed chains in systems containing more than two chain lengths. The calculated molecular weight distributions of surface-adsorbed macromolecules are listed in Table II. Calculated values agree closely with the numbers obtained from the simulation except when large numbers of chain length 10 are present (sample 1). The simulation value is lower than predicted when a large proportion of short chains are present due to the trapping effect noted above.

Table III
R_g and L for Reversible and Irreversible Binding[a]

P_R	no. of adsorbed chains	R_g	L
0.00	159	2.24	5.06
0.25	137	2.22	4.54
0.50	132	2.24	4.58

[a] $P_{A-A} = 1.0$, $\chi_{AS} = \chi_{BS} = 0.0$, number of free chains = 20, chain length = 20.

Up to this point, all results presented have assumed irreversible binding. As described earlier, the feature of reversibility is introduced by prescribing a probability P_R, which reflects the ease of desorption (or dissociation from the layer) for labile chains. Higher values of P_R correspond to an increased probability of desorption or dissociation. As intuitively expected, increasing P_R from 0.0 to 0.5 should decrease the number of bound chains. However, the effect is negligible in the first layer: surface coverage decreases by only approximately 2%. Table III, on the other hand, gives the total number of adsorbed chains at four million time steps for $P_R = 0.0$, 2.5, and 0.50. Here, it can be seen that introducing reversibility does in fact significantly decrease the number of chains bound in the outer layers of the interfacial region.

Table III also shows the effect of increasing P_R on R_g and L of the adsorbed chains. We are below the C^* surface concentration in the reversible simulations after four million steps, and the values of R_g are what would be expected in the regime of nonoverlapping adsorbed coils ($R_g \sim N^{3/5}$). The measured layer thickness for chain length 20 when binding is reversible was somewhat less than the layer thickness in the irreversible simulations, but it is still greater than R_g.

Conclusions

In this paper, we have shown that self-assembly in triblock copolymers affects the behavior of these chains near an interface. In particular, self-association affects the extent of surface coverage, as well as the microstructure of the interfacial region. We have also shown that the morphology of this interfacial region is significantly dif-

ferent than that for diblocks or terminally attached homopolymers.

Our observations are particularly useful in choosing an appropriate polymer for such applications as steric stabilization of dispersed particles. The results indicate that a dilute concentration of relatively short polymers many provide the ideal agents for this function. Under these conditions, the chains would adsorb in loop conformations, with both stickers bound to the surface. Subsequent interactions between the hydrophilic segments on neighboring particles would prevent flocculation. The triblock architecture may provide a significant advantage over the diblock structure since the presence of two stickers ensures that the chains are more securely bound to the surface.

The effects of self-associations on surface adsorption may be even more significant for more complex amphiphilic architectures, such as the comb- or dog-boned-shaped structures that are widely used for a variety of industrial processes.[1] Our future work will focus on the surface adsorption of these complicated amphiphilies.

Acknowledgment. We thank Dr. James E. Brady, Dr. Robin Garrell, and Dr. Chris Lantman for their illuminating comments and suggestions concerning this work. A.C.B. gratefully acknowledges financial support from the following sources: the National Science Foundation, through Grant DMR-8718899; the donors of the Petroleum Research Fund, administered by the American Chemical Society; and the Union Carbide Corporation.

References and Notes

(1) Hancock, R. I. In *Surfactants*; Tadros, Th. F., Ed.; Academic Press: London, 1984; p 287.
(2) Tanford, C. *The Hydrophobic Effect: Formation of Micelles and Biological Membranes*; Wiley & Sons: New York, 1973.
(3) Leibler, I.; Orland, H.; Wheeler, J. *J. Chem. Phys.* **1983**, *79*, 3350.
(4) Marques, C.; Joanny, J. F.; Leibler, L. *Macromolecules* **1988**, *21*, 1051.
(5) van Lent, B.; Scheutjens, J. M. H. M. *Macromolecules* **1989**, *22*, 1931.
(6) Tassin, J. F.; Siemens, R. L.; Tang, W. T.; Hadziioannou, G.; Swalen, J. D.; Smith, B. A. IBM Research Report. RJ 6252 (61649); 1988.
(7) Larson, R. G.; Scriven, L. E.; Davis, H. T. *J. Chem. Phys.* **1985**, *83*, 2411.
(8) Larson, R. G. *J. Chem. Phys.* **1988**, *89*, 1642.
(9) Balazs, A. C.; Anderson, C.; Muthukumar, M. *Macromolecules* **1987**, *20*, 2411.
(10) Verdier, P. H.; Stockmayer, W. H. *J. Chem. Phys.* **1962**, *36*, 227.
(11) Hilhorst, J. H.; Deutch, J. M. *J. Chem. Phys.* **1975**, *63*, 5153.
(12) Granick, S. American Physical Society Meeting, March 1989; High Polymer Physics Division, Poster Session.
(13) Flory, P. J. *Principles of Polymer Chemistry*; Cornell University Press: Ithaca, NY, 1953.
(14) de Gennes, P.-G. *Scaling Concepts in Polymer Physics*; Cornell University Press: Ithaca, NY, 1979; p 77.
(15) Alexander, S. *J. Phys. (Paris)* **1977**, *38*, 983.
(16) de Gennes, P.-G. *Macromolecules* **1980**, *13*, 1069.
(17) Patel, S.; Tirrell, M.; Hadziioannou, G. *Colloids Surf.* **1988**, *31*, 157.
(18) Tirrell, M., private communication.
(19) Munch, M. R.; Gast, A. P. *Macromolecules* **1988**, *21*, 1366.
(20) Cosgrove, T.; Heath, T.; van Lent, B.; Leermakers, F.; Scheutjens, J. *Macromolecules* **1987**, *20*, 1962.
(21) de Gennes, P.-G. *Scaling Concepts in Polymer Physics*; Cornell University Press: Ithaca, NY, 1979; p 176.